MORPHOLOGICAL CHANGES IN THE MICROSTRUCTURE IN NEW HIGH MO SUPER FERRITIC STAINLESS STEELS*

Lorena Braga Moura[1]
Mohammad Masoumi[2]
Francisco Evaristo Uchoa Reis[3]
Alexander Catunda Carneiro[4]
Lucas Sousa Félix[5]
Hamilton Ferreira Gomes de Abreu[6]

Abstract

High Mo content in stainless steels improves the resistance to naphthenic corrosion in equipment used in the processing of heavy crude oil. However, causes the precipitation of intermetallic phases such as Sigma (σ), Chi (χ) and Mu (μ), nitrides ($Fe_5Mo_{13}N_4$), carbides [$(Cr, Fe, Mo)_{23}C_6$] or Nb and Ti carbonitrides [Nb(CN) and Ti(CN)]. These precipitations result in embrittlement, decreased corrosion resistance at elevated temperatures, and reduced toughness. Experimental alloys of superferritic stainless steel (25% Cr-X% Mo-Y% Ni) with (X = 5 and 7%) and (Y = 2 and 4%) with additional Ti and Nb were developed. The effect of Mo contents higher than those of the known commercial alloys was studied. The influence of the chemical composition variation on the kinetics precipitation of intermetallic phases and evaluated effects on the microstructural characteristics and mechanical properties were analyzed. The σ phase was formed before the χ phase in the samples treated at 600°C and 700°C. However, at higher temperatures of 800 ° C and 900 ° C, the χ phase precipitated earlier than the σ phase. The formation of Gamma (γ) phase in samples with more Ni occurred by eutectoid reaction (α → σ + γ) in the form of lamellar agglomerates.

Keywords: Superferritic stainless steel; High molybdenum; Phases transformations.

1 *Engineering and Materials, PhD, Professor / Industry department, IFCE, Fortaleza, Ceara, Brazil.*
2 *Engineering and Materials / PhD, Metallurgical Engineering department, UFC, Fortaleza, Ceara, Brazil*
3 *Engineering and Materials, DSc, Professor/Mechanical Engineering department, UFERSA, Mossoró, Rio Grande do Norte, Brazil.*
4 *Mechanical technician, student, Industry department, IFCE, Fortaleza, Ceara, Brazil.*
5 *Mechanical technician, student, Industry department, IFCE, Fortaleza, Ceara, Brazil*
6 *Engineering and Materials /PhD, professor/Metallurgical Engineering department, UFC, Fortaleza, Ceara Brazil.*

** Technical contribution to the 74º Congresso Anual da ABM – Internacional, part of the ABM Week 2019, October 1st-3rd, 2019, São Paulo, SP, Brazil.*

1 INTRODUCTION

The development of ferritic stainless steel in petroleum industry has received considerable attention in the last decade [1-5]. In the current study, novel alloys were designed with a content of Cr up to 25 wt% and Mo between 5–7 wt % to improve naphthenic corrosion and pitting resistance in the chlorides containing environment. Others elements like carbon (C) and nitrogen (N) were kept low mainly to have a good ductility and weldability. Nickel (Ni) was added to increase toughness and niobium (Nb) and titanium (Ti), carbide formers, were added to ensure that the material presented a ferritic matrix and formed carbides and nitrides that act in the grain refining [6-9]. Similar alloys but with a smaller amount of Mo have been used in many corrosive environments such as those in the chemical, petroleum refining, petrochemical, food processing, paper manufacturing and heat-sealing industries, and in marine applications [10;11].

The high concentration of alloying elements in stainless steels (austenitic, ferritic, duplex and high performance) affects the microstructural stability causing the precipitation of intermetallic phases such as Sigma (σ), Chi (χ) and Laves (η). They are the three intermetallic phases most frequently found in stainless steels [4, 6, 12, 13]. Also, the Mu (μ) phase precipitates in steels containing higher molybdenum contents [3, 5]. The σ-phase is often observed in various series of stainless steels. It is a tetragonal crystal structure, and its precipitation temperature is between 600°C and 1000°C [14-15]. The χ-phase may occur in austenitic, ferritic, and duplex stainless steels and its precipitation is also associated with negative effects on corrosion and mechanical properties. In stainless steels, the precipitation of nitrides ($Fe_5Mo_{13}N_4$), carbides $(Cr, Fe, Mo)_{23}C_6$ or carbonitrides (Nb(C, N) and Ti (C, N)) may also occur [16,17,18]. Such precipitation phenomena result in loss of toughness, ductility and corrosion resistance of the steel. Apart from the precipitation of all these deleterious phases, the superferritic stainless steels are susceptible to austenite precipitation during heat treatment in the temperature range of 500°C to 950°C, depending on the concentration of Ni [6,9].

The present work investigates the morphological changes in the microstructure and its influence on the mechanical properties in experimental superferritic stainless steels when these alloys were exposed to temperatures between 600 and 900oC for different periods of time.

2 MATERIALS AND METHODS

Three ingots with different compositions were forged. Table. 1 shows the identification and chemical composition of each alloy.

Table 1. Chemical Composition (wt.%) of experimental

Alloys	C	Cr	Mo	Ni	Ti	Nb	N
5Mo4Ni	0.05	25.3	5.8	3.9	0.01	0.2	0.06
7Mo2Ni	0.05	24.6	7.6	1.8	0.01	0.3	0.06
7Mo4Ni	0.05	25.4	7.3	4.2	0.03	0.2	0.06

Samples measuring 15mm x 10mm x 4mm from each ingot were solution annealed at 1080 °C (5Mo4Ni) and 1180°C (7Mo2Ni and 7Mo4Ni) for 15 minutes and quenching in water. Isothermal heat treatments were performed in order to induce precipitation in temperatures from 600°C to 900°C in times ranging from 15 minutes to 100 h. All samples were water quenching after heat treatment.

The microstructural evolution of the samples was analysed using several complementary analysis techniques, such as Optical Microscopy (OM), Scanning Electron Microscopy (SEM) along with chemical microanalysis by Energy Dispersive Spectrometry (EDS) and X-ray diffraction (XRD). To associate microstructure changes with mechanical properties, Vickers microhardness (HV) was performed.
Samples were prepared using conventional metallographic preparation. They were examined by OM and SEM after etching in Behara etchant (23 mL HCl; 0.35g $K_2S_2O_5$ and 77 mL distilled water) heated to 60°C, followed by electrolytic etching using 2 V for 10 s in a 40% HNO_3 aqueous solution [19]. X-ray diffraction was performed with CuKα radiation, equipped with monochromator and 0.01° step. The XRD measurements were refined by the Rietveld method [20]. Vickers hardness (HV) measurements were performed with 0.1 kgf load and time of 10 s.

3 RESULTS AND DISCUSSION

3.1. Microstructural Evolution

Changes in the microstructure were observed by subjecting the material to heat treatments where the temperature and the time of exposure to these temperatures were varied. The solution annealed samples presented grain boundary free of precipitates and completely ferritic matrix with fine and dispersed stabilized carbides. After heat treatment (Figure 1), the 5Mo4Ni alloy increased the phase precipitation in the form of plates in the grain boundary and in the ferritic matrix. Some precipitates in the matrix presented coarse dendritic morphology that evolved forming agglomerates of lamellar phases close to the grain boundary.
For the 7Mo2Ni alloy, some precipitates showed elongated plates morphology in the grain boundary and in the matrix. For the 7Mo4Ni alloy, high aging temperature increased the amount of lamellar phase precipitated. Comparing the alloys with 7% Mo treated at 800 °C for 10h (Figure 1b-c) it was observed that the increase of 2% Ni to 4% Ni favored the appearance of lamellar morphology. The phase with lamellar morphology was similar to the morphology found in duplex steels caused by a eutectoid reaction of the type δ → σ + γ. The presence of Ni in the composition provides formation of γ-phase adjacent to σ-phase. The depletion of Cr and Mo and the presence of Ni in areas close to σ-phase decrease the stability of ferrite and they are replaced by γ-phase [21].

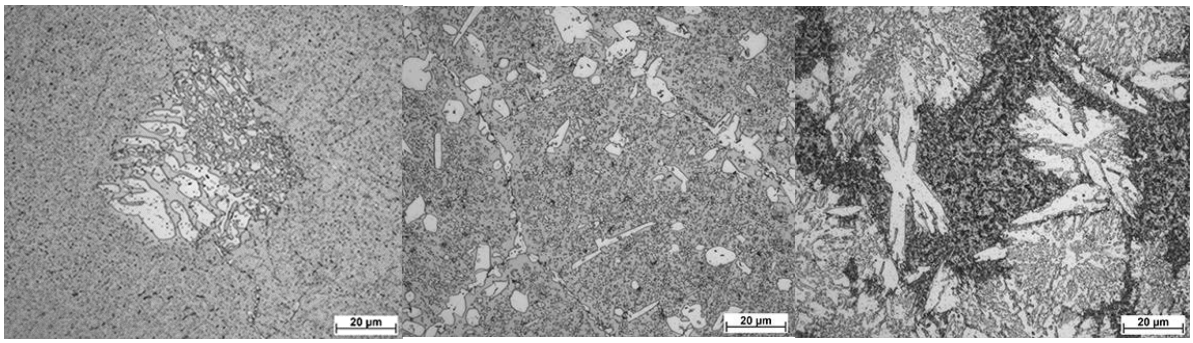

(a) (b) (c)

Figure 1. OM samples aged for 10 hours at 800°C a) 5Mo4Ni; b) 7Mo2Ni and c) 7Mo4Ni.

In all experimental alloys, the phase precipitation occurred initially in the grain boundary, triple points and dispersed points in the matrix. With the variation of the

heat treatment time, phases precipitate growing towards the matrix. Figure 2 shows the evolution of 5Mo4Ni alloy aged at 900°C for 1 h, 5 h and 10 h.

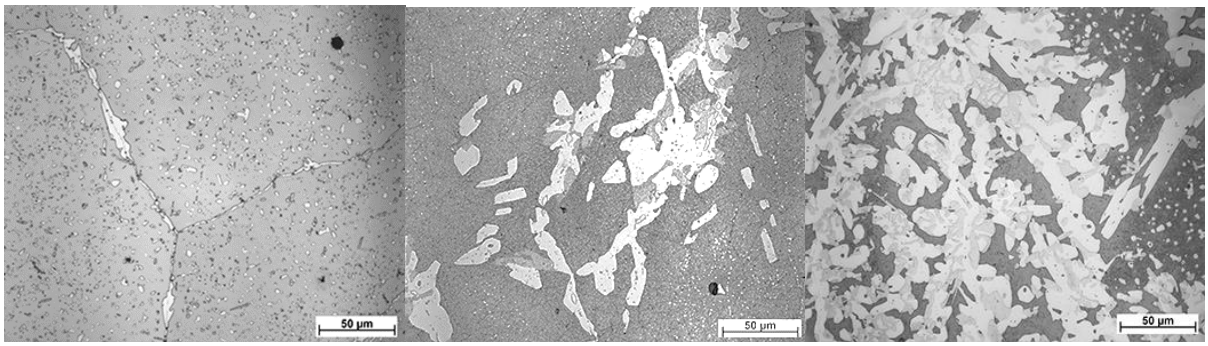

(a) (b) (c)

Figure 2. Microstructural evolution of 5Mo4Ni alloy aged at 900°C a) 1 h; b) 5 h; c) 10h.

The SEM image (Figure 3a) highlights the coarse dendritic precipitation in the 5Mo4Ni alloy heat treated at 800°C for 10 h. EDS analysis identified γ-phase forming the lamellar agglomerates composed of γ-phase plates involved by σ-phase. The χ-phase appears in smaller quantities within the σ-phase and dispersed in the matrix. The composition of the α-phase within the agglomerates has lower alloying elements when compared to α-phase located outside the lamellar agglomerates. EDS analysis for 7Mo2Ni alloy identified χ-phase precipitation inside the elongated plates of σ-phase in the grain boundary (Figure 3b). The increase in temperature reduced the Mo content in the χ-phase composition from 22.7%wt Mo at 700°C to 10.5%wt Mo at 900°C. It did not have the γ-phase formation in this alloy result that is in accordance with Thermo-Calc calculations published in Moura et al, 2013 [4].

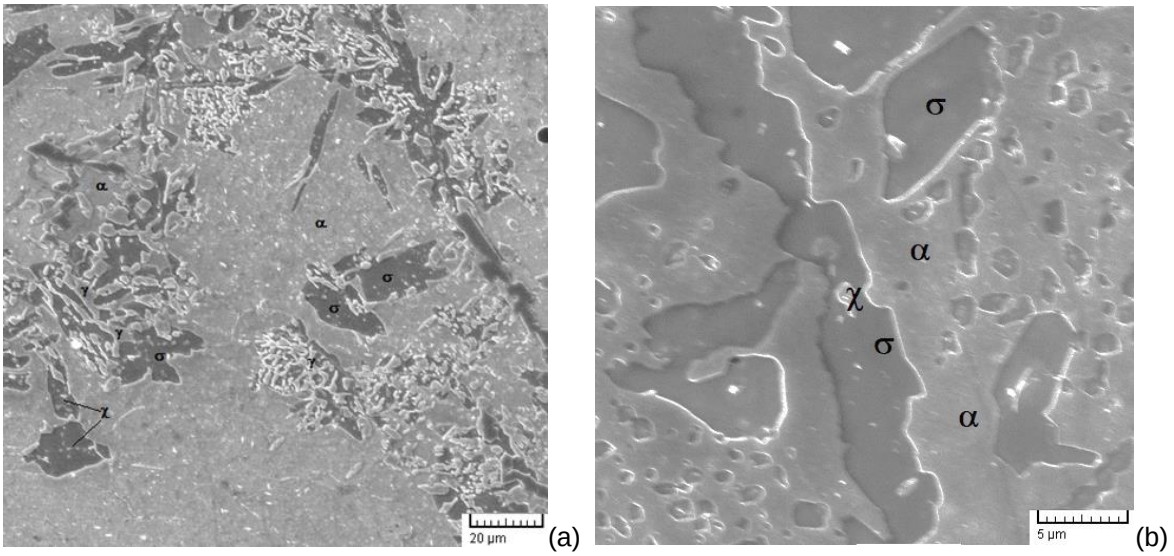

(a) (b)

Figure 3. SEM image and EDS analysis of the phases of the alloys heat treated at 800 ° C for 10h. a) 5Mo4Ni b) 7Mo2Ni

SEM image and EDS analysis (Figure 4a-b) of the precipitated phases and microstructural evolution in the 7Mo4Ni alloy aged at 900 °C for 1 h and 10 h, identified that the dendritic regions are formed by σ-phase, are rich in Cr and Mo, involve regions with high Ni content, and indicate the formation of γ-phase. After 10 h

of heat treatment at 900 °C, The reduction in the quantity of α-phase was followed by the increase of precipitated σ and γ-phases quantities. Phases morphology and evolution of precipitations showed notable characteristics of a eutectoid reaction.

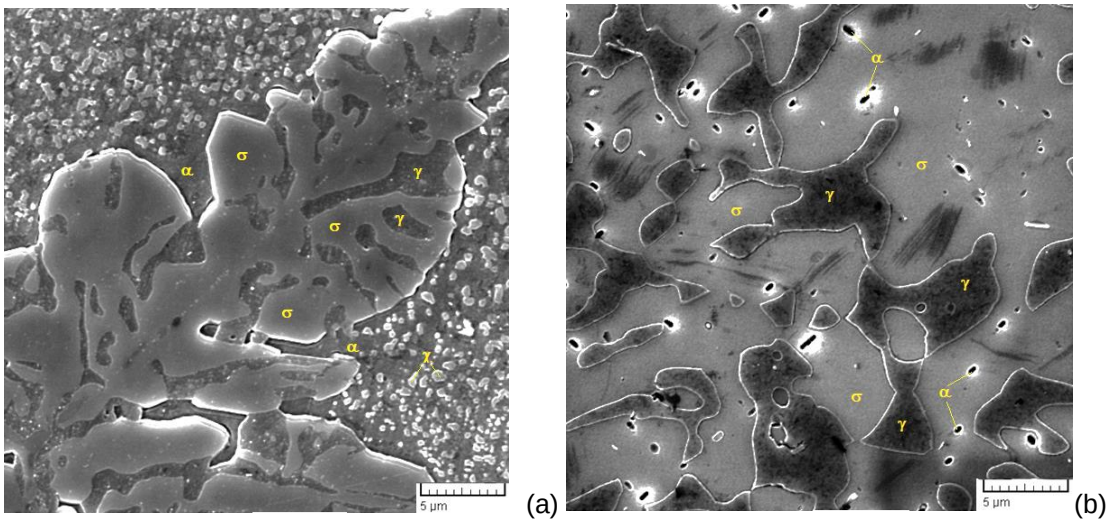

Figure 4. SEM image and EDS analysis of the phases of the alloys heat treated at 800 ° C for 10h. a) 5Mo4Ni b) 7Mo2Ni

The kinetics of phase precipitation with respect to composition, temperature and treatment time variation were studied using XRD measurements (with Rietveld refinement). XRD patterns measurements in all alloys heat treated at 600 °C only α and σ-phases was detected and confirmed by SEM / EDS analyzes. In the alloys with 4% Ni treated at 700 °C, the presence of γ-phase was observed. In the 5Mo4Ni alloy, the γ-phase was detected after 100 h of treatment, while for the 7Mo4Ni alloy the γ-phase was detected after 10h of heat treatment. This increase in γ-phase kinetics in the 7Mo4Ni alloy may be related to the higher amount of σ-phase precipitated in this alloy which favours the formation of γ-phase that is formed in the depleted regions of Cr and Mo. The precipitation of σ-phase occurred in all alloys, for the alloys with 7% Mo it occurred after 15 minutes, while for the 5Mo4Ni alloy the σ-phase precipitated after 30 minutes of heat treatment. The increase of Mo content from 5% Mo to 7% Mo accelerates the kinetics precipitation of the σ-phase. The increase in temperature from 600 °C to 700 °C favored precipitation of the χ-phase after 5 h of treatment. Figure 5 shows the diffractogram of the 5Mo4Ni alloy treated at 900°C between 1 h and 100 h in the interval 2θ between 35 and 55 °. The dissolution of the χ-phase, the increase of the amount of σ-phase and the increase of the precipitation of the γ-phase after 100 h of heat treatment, accompanied by the reduction of the intensity of the ferrite peaks, were highlighted.

Raising the temperature from 700 °C to 800 °C accelerated γ-phase precipitation at the 5Mo4Ni alloy started after 10 h at 800 °C and at 7Mo4Ni alloy after 5 h at 800 °C. For samples heat treated at 800 °C and 900 °C, between 1 h and 10 h, increased the amount of χ-phase and reduced the amount of σ-phase precipitated. For alloys treated at 900 °C, the kinetics of phase transformation in the 7Mo4Ni alloy was higher than that observed for the other alloys studied. The 7Mo2Ni alloy presented lower transformation kinetics after 10 h of treatment and lesser amount of secondary phase precipitated compared to 4% Ni alloys (Figure 6).

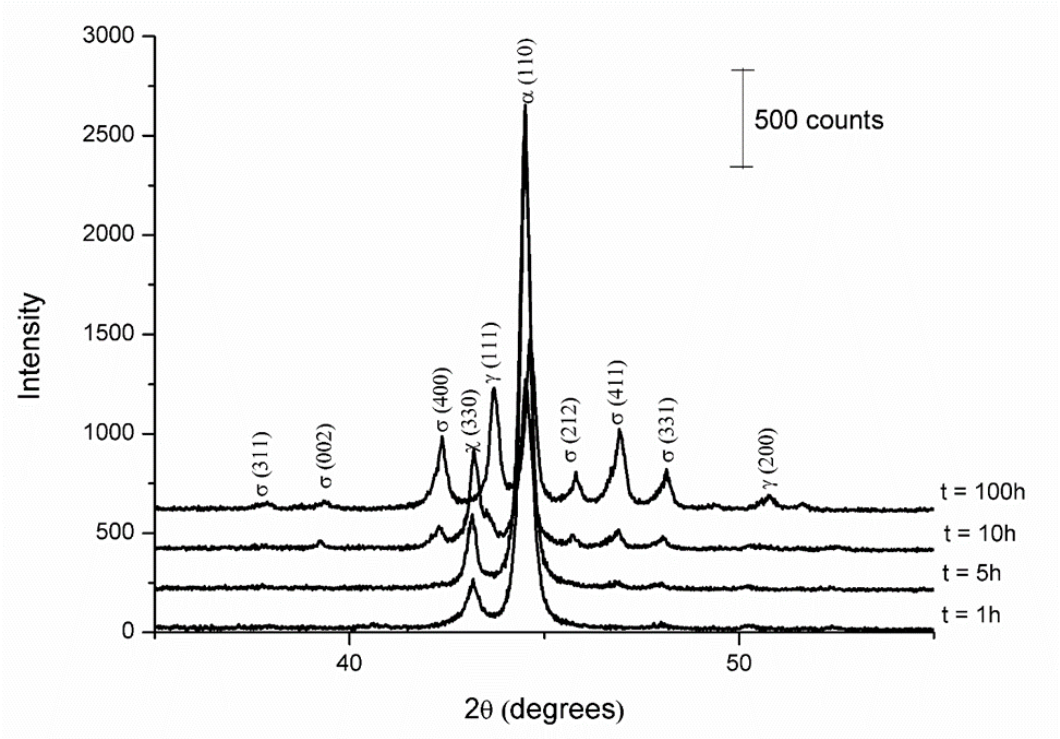

Figure 5. XRD patterns to 5Mo4Ni alloy treated at 900°C at various time

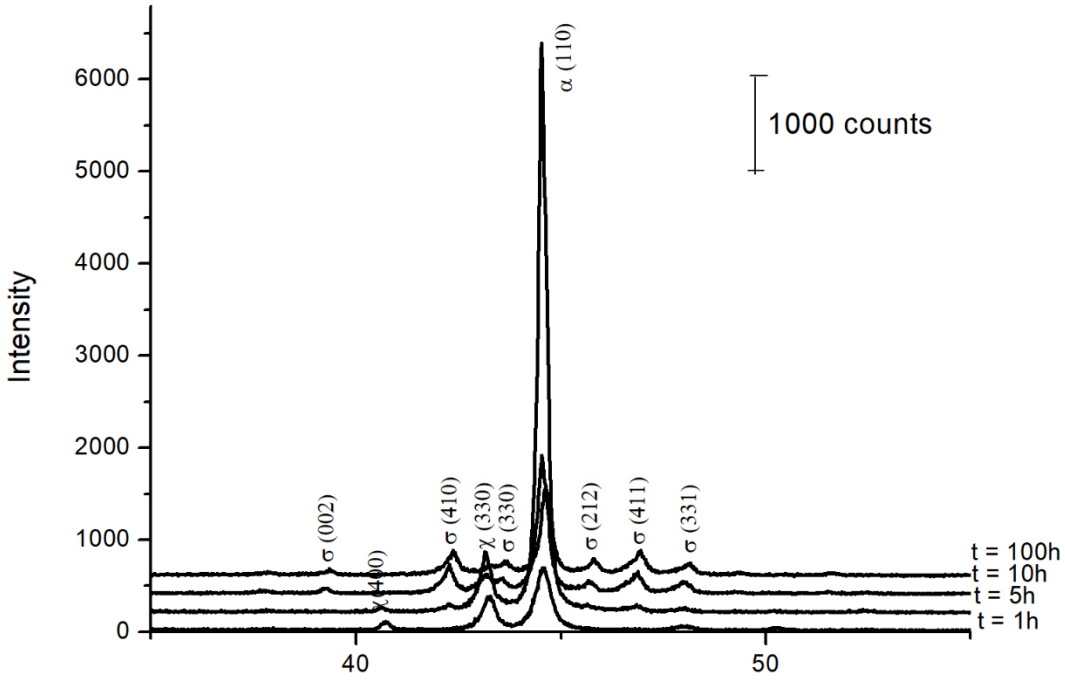

Figure 6. XRD patterns to 7Mo2Ni alloy treated at 900°C at various time

The curves of phases precipitated for the 5Mo4Ni alloy were compared with the hardness measurements (Figure 7a-b). It was observed that the hardness increase is related to the increase in the amount of deleterious phases precipitated in all alloys studied. The hardness reduction, in 5Mo4Ni alloy, was observed in the range of 30 minutes to 5 hours of the sample treated at 900 °C which coincides with the reduction

of the amount of σ-phase precipitated. A higher amount of γ-phase in samples heat treated at 900 °C for 100 h resulted in the reduction of hardness 561 HV at 900 °C, when compared to samples heat treated at 700 °C (601 HV) and 800 °C (606 HV). The reduction of hardness after heat treatment at 800 °C for 10 h can be related to the onset of γ-phase transformation.

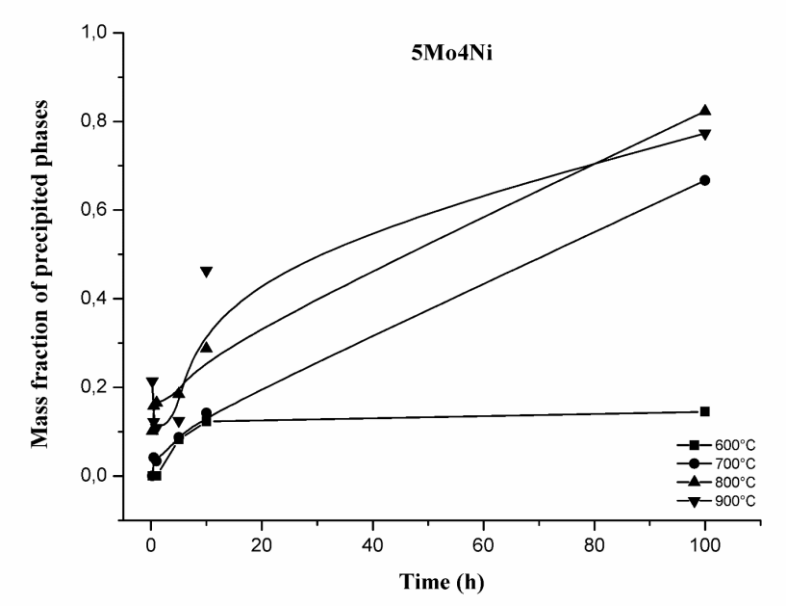

(a)

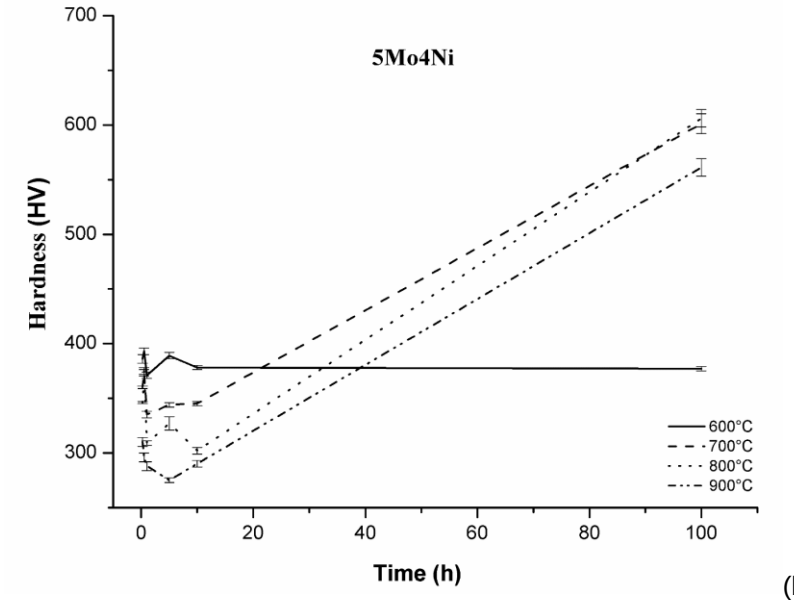

(b)

Figure 7. Comparison between phase precipitation (a) and hardness (b) as a function of the isothermal treatment in the 5Mo4Ni alloy

For the 7Mo2Ni alloy, the maximum hardness occurred at 700 °C /100 h (594 HV), exactly in the condition of greater precipitation of deleterious phases. In the 7Mo4Ni alloy at 900°C/100 h (687 HV) with increasing amount of transformed γ-phase, the hardness was lower than the samples heat treated at 700°C (717 HV) and 800°C (770 HV).

In the present work, the hardness increase related to the precipitation of σ and χ-phases and the reduction of hardness associated with austenite transformation were observed. The relationship between the increase in the amount of intermetallic phase

(σ and χ phases) and the hardness increase was also observed previously in AISI 444 ferritic stainless steels treated between 560°C and 800°C 41.

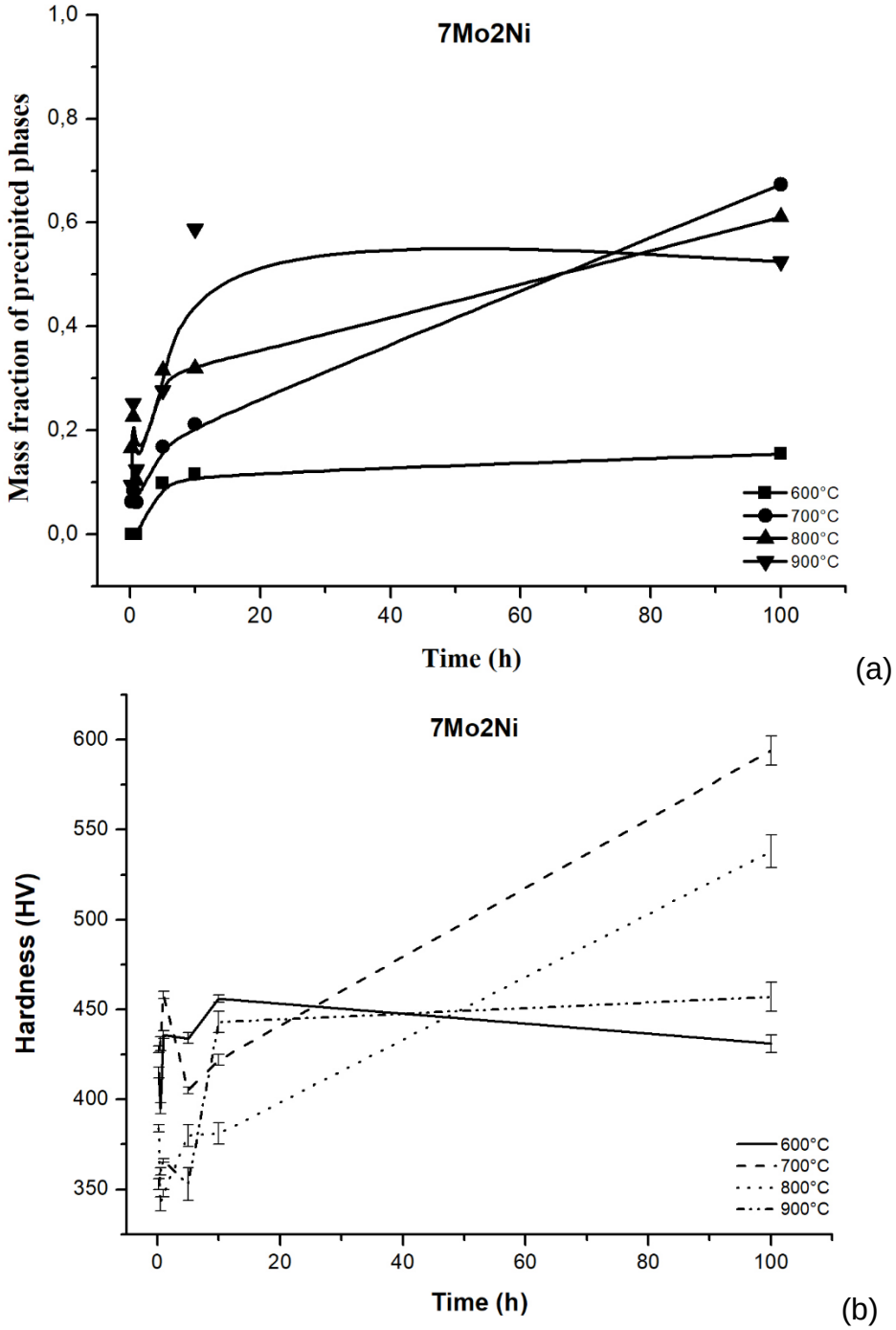

Figure 8. Comparison between phase precipitation (a) and hardness (b) as a function of the isothermal treatment in the 7Mo2Ni alloy

4 CONCLUSION

This study involved the phases present in novel FeCrNi with high contents of Mo in the temperature range from 600 °C to 900 °C for different periods of time. For alloys heat treated at temperatures of 600°C and 700°C, the σ-phase formed before the χ-phase. For higher temperatures of 800 °C and 900 °C, the χ-phase precipitated after

15 minutes of treatment, before the σ-phase, which precipitated only after 5 h of treatment.
In the 5Mo4Ni alloy (alloy with less Mo) *σ*-phase precipitation started in the contour of grain with elongated shape and inside the grain in the form of faceted plates. Within the grain, the *σ*-phase evolved to the formation of dendrites that grew to form lamellar agglomerates. In the 7Mo2Ni alloy, *σ*-phase precipitation occurred first in the grain boundary and triple points. In the 7Mo4Ni alloy, the *σ*-phase precipitated in the grain boundaries forming small regions in the form of rounded plates and in the ferritic matrix with elongated morphology or faceted plates.
For the 4% Ni content alloys, *γ*-phase occurred by eutectoid reaction (α → σ + γ), forming lamellar agglomerates. The 7Mo4Ni alloy had a higher precipitation rate and a higher amount of secondary phases precipitated in the range of 600 °C to 900 °C. The phase precipitation rates of the 5Mo4Ni and 7Mo2Ni alloys at 600 °C and 700 °C were similar. The 7Mo2Ni alloy showed a lower precipitation rate and the lower amount of phases precipitated at 800 °C and 900 °C after heat treated for 10 h. For 4% Ni content alloys, the presence of γ-phase caused the reduction in the hardness. The 7Mo2Ni alloy presented lower hardness compared to other alloys treated between 600 °C and 900 °C.

Acknowledgments

The authors wish to acknowledge the financial support for this research from FUNCAP (Fundação Cearense de Apoio ao Desenvolvimento Científico e Tecnológico). The authors would specially like to thank Mr. Oscar Gonzales, Metallurgist and Director of FAINOX (Fundição de Aços Inoxidáveis – São Paulo, Brazil) generous supplied the experimental superferritic stainless steels used for this study.

REFERENCES

1 ABREU, H. F. G. D.; BRUNO, A. D. S.; TAVARES, S. S. M.; SANTOS, R. P.; CARVALHO, S. S. Effect of high temperature annealing on texture and microstructure on an AISI-444 ferritic stainless steel. Materials Characterization, v. 57, p. 342–347, 2006.
2 SOUZA, J. A.; ABREU, H. F. G.; NASCIMENTO, A. M.; DE PAIVA, J. A. C.; DE LIMA-NETO, P.; TAVARES, S. S. M. Effects of Low-Temperature Aging on AISI 444 Steel. Journal of Materials Engineering and Performance, v. 14, n. 3, p. 367-372, 2005.
3 MOURA, L. B.; GUIMARÃES, R. F.; ABREU, H. F. G.; MIRANDA, H. C.; TAVARES, S. S. M. Naphthenic Corrosion Resistance, Mechanical properties and microstructure evolution of experimental Cr-Mo steels with high Mo content. Materials Research, v.15, n.2, p.277-284, 2012.
4 MOURA, L. B.; DE ABREU, H. F. G.; NEGREIROS, Y. S. Computational thermodynamic analysis of secondary phases in super ferritic stainless steels. Journal of Materials Research and Technology, v. 2, n. 3, p. 282-287, 2013.
5 GOMES DA SILVA, M. J.; HERCULANO, L. F. G.; URCEZINO, A. S. C.; ARAÚJO, W. S.; DE ABREU, H. F. G.; DE LIMA-NETO, P. Influence of Mo content on the phase evolution and corrosion behavior of model Fe–9Cr–xMo (x = 5, 7, and 9 wt%) alloys. Journal of Materials Research, v. 30, n. 12, p. 1999-2007, 2015.
6 ANDRADE, T. F. D.; KLIAUGA, A. M.; PLAUT, R. L.; PADILHA, A. F. Precipitation of Laves phase in a 28%Cr–4%Ni–2%Mo–Nb superferritic stainless steel. Materials Characterization, v. 59, n. 5, p. 503-507, 2008.

7 XU, W.; SAN MARTIN, D.; RIVERA DÍAZ DEL CASTILLO, P. E. J.; VAN DER ZWAAG, S. Modelling and characterization of chi-phase grain boundary precipitation during aging of Fe–Cr–Ni–Mo stainless steel. Materials Science and Engineering: A, v. 467, n. 1-2, p. 24-32, 2007.

8 DOWLING, N. J. E.; KIM, H.; KIM, J.-N.; AHN, S.-K.; LEE, Y.-D. Corrosion and Toughness of Experimental and Commercial Super Ferritic Stainless Steels. Corrosion Nace International, v. 55, n. 8, p. 743-755, 1999.

9 NG, P. G.; CLARKE, E.; KHOO, C. A.; FOURLARIS, G. Microstructural evolution during aging of novel superferritic stainless steel produced by the HIP process. Materials Science and Technology, v. 22, n. 7, p. 852-858, 2006

10 RICHAUD-MINIER, H.; PASCAL, G.; MARCHEBOIS, H.; SCHUMERTH, D. Titanium and super stainless for seawater cooled heat exchangers. Stainless Steel World, Netherlands, p. 32-38, 2008. Available on: < http://www.desalination-world.com/pdf/p7011.pdf >. (Cited 2013, May 02)

11 TVERBERG, J. C.; JANIKOWSKI, D. S. The Performance of Superferritic Stainless Steels in High Chloride Waters. USA, p. 8, 2005. Available on: < http://www.plymouth.com/media/13951/SSW%20Oct%2005%20Perf%20of%20Superferritic%20SS%20in%20High%20Chloride%20.pdf >. (Cited 2013, March 30)

12 PARDAL, J. M.; TAVARES, S. S. M.; FONSECA, M. D. P. C.; SOUZA, J. A. D.; VIEIRA, L. M.; ABREU, H. F. G. D. Deleterious Phases Precipitation on Superduplex Stainless Steel UNS S32750: Characterization by Light Optical and Scanning Electron Microscopy. Materials Research v. 13, n. 3, p. 401-407, 2010.

13 PIMENTA JR., F. C.; REICK, W.; PADILHA, A. F. Comparative Study between Precipitation of the Sigma Phase in a Superferritic Stainless Steel and a Duplex Stainless Steel (In Portuguese). In: 14ª CBECiMat - Brazilian Congress of Materials Engineering and Science, 2000, São Pedro - SP. p.301-309

14 HSIEH, C.-C. and WU, W. Overview of Intermetallic Sigma (σ) Phase Precipitation in Stainless Steels, ISRN Metallurgy, v. 2012, p. 1-16, 2012.

15 VILLANUEVA, D. M. E.; JUNIOR, F. C. P.; PLAUT, R. L.; PADILHA, A. F. Comparative study on sigma phase precipitation of three types of stainless steels: austenitic, superferritic and duplex. Materials Science and Technology, v. 22, n. 9, p. 1098-1104, 2006.

16 ESCRIBA, D.M., MATERNA-MORRIS, E., PLAUT, R.L., PADILHA, A.F., Chi-phase precipitation in a duplex stainless steel, Materials Characterization, v. 60, n. 11, p.1214-1219, 2009.

17 BROWN, E. L.; BURNETT, M. E.; PURTSCHER, P. T.; KRAUSS, G. Intermetallic phase formation in 25Cr-3Mo-4Ni ferritic stainless steel. Metallurgical Transactions A, v. 14, n. 4, p. 791-800, 1983

18 PARK, C. J.; AHN, M. K.; KNOW, H. S. Influence of Mo substitution by W on the precipitation kinetics of secundary phases and the associated localized corrosion and embrittlement in 29%Cr ferrite stainless steels. Materials Science andEngineering, v. 418, n. 1-2, p. 211-217, 2006

19 BARROS, I. F. D. Dissimilar welding of AISI 444 ferritic stainless steel and AISI 316 austenitic stainless steel by means of the autogenous TIG process using pulsed current.2014. 195p. (MSc thesis) (In Portuguese). Materials and Metalurgical Department, UFC, Fortaleza, Brazil, 2014

20 YOUNG, R. A. The Rietveld Method. New York: Oxford University Press: 1995. 192 p

21 KRAUSS, G. Steels: Heat Treatment and Processing Principles**,** ASM International**,** January, 1990.